



**HAL**  
open science

## Development and characterization of thermal insulation materials from renewable resources

M. Viel, F. Collet, Christophe Lanos

### ► To cite this version:

M. Viel, F. Collet, Christophe Lanos. Development and characterization of thermal insulation materials from renewable resources. *Construction and Building Materials*, 2019, 214, pp.685-697. 10.1016/j.conbuildmat.2019.04.139 . hal-02182004

**HAL Id: hal-02182004**

**<https://univ-rennes.hal.science/hal-02182004>**

Submitted on 22 Oct 2021

**HAL** is a multi-disciplinary open access archive for the deposit and dissemination of scientific research documents, whether they are published or not. The documents may come from teaching and research institutions in France or abroad, or from public or private research centers.

L'archive ouverte pluridisciplinaire **HAL**, est destinée au dépôt et à la diffusion de documents scientifiques de niveau recherche, publiés ou non, émanant des établissements d'enseignement et de recherche français ou étrangers, des laboratoires publics ou privés.



Distributed under a Creative Commons Attribution - NonCommercial 4.0 International License

# Development and characterization of thermal insulation materials from renewable resources

Marie Viel<sup>a,b,\*</sup>, Florence Collet<sup>a</sup>, Christophe Lanos<sup>a</sup>

<sup>a</sup> *Université de Rennes, Laboratoire Génie Civil et Génie Mécanique, BP 90422, Rennes, France*

<sup>b</sup> *Université de Nantes, Institut de recherche en Génie Civil et en Génie Mécanique, BP 92208, Nantes, France*

---

## Abstract

The present study has investigated the scope for valuation of agro-resources by-products as aggregates and as binding material to produce rigid fully bio-based composite panels. Two types of aggregates: hemp shiv and corn cob residues (obtained after alkali treatment on the corn cob), and six types of green binders are investigated. Specimens are produced to verify the gluing effect, to characterize mechanical, thermal and hygric properties of developed composites and to identify the best aggregate-binder mixture. They show interesting thermal conductivity ranging from 67 to 148 mW/(m.K) at dry state, excellent hygric properties ( $MBV > 2 \text{ g}/(\text{m}^2 \cdot \%RH)$ ) and high enough mechanical properties to be self bearing. These results suggest that developed composites can be used as building materials but not for the same types of use. In fact, some composites would be more suitable for thermal insulating products and others would be better suited for indoor facing panels.

*Keywords:*

Agricultural waste valuation, Hemp shiv, Corn cob, Green binder, Hygrothermal characterization, Mechanical properties

---

\*Corresponding author

*Email addresses:* [marie.viel@univ-nantes.fr](mailto:marie.viel@univ-nantes.fr) (Marie Viel), [florence.collet@univ-rennes1.fr](mailto:florence.collet@univ-rennes1.fr) (Florence Collet), [christophe.lanos@univ-rennes1.fr](mailto:christophe.lanos@univ-rennes1.fr) (Christophe Lanos)

## 1. Introduction

Nowadays, the building sector is one of the three most energy consuming sectors with industry and transport, particularly because of heating, ventilation and air conditioning systems that ensure indoor thermal comfort. So, building well insulating buildings is important to save energy more efficiently, in particular by reducing heat transfer through the envelopes [1, 2, 3]. Hence, there is a high demand for renewable, environmentally friendly, low cost and high thermal resistance insulation materials [2]. One way to address these objectives is the development of green insulating materials to replace conventional ones [4].

A bio-based material is a material obtained from raw material of mainly biological origin, preferably requiring very little processing. Fossil resources are excluded, so materials from renewable biomass animal or plant are mainly considered.

This type of material can lead to excellent hygrothermal performance. They have the ability to moderate humidity of the indoor air by adsorbing and desorbing water vapor which allows to reduce the ventilation rate and thus, the need for heating in winter and for air conditioning in summer [5, 6].

Moreover, they are renewable and environmentally friendly unlike some traditional thermal insulators such as mineral wool which have poor environmental performance. Indeed, various pollutants such as  $\text{CO}_x$ ,  $\text{NO}_x$ ,  $\text{SO}_x$ , volatile organic compounds and particles are emitted during their energy-intensive production [2, 4]. The most commonly used bio-based materials are wood, straw, hemp, corn, or sheep wool. Even if wood is the most developed and able to compete with traditional insulation materials, other materials are used more and more, such as cellulose wadding or hemp concrete [2, 5, 4].

This study investigates the development of fully bio-based composites to be used to produce rigid insulating panels. Firstly, six green binders are used. Two bio-binders are developed, they are obtained by the extraction process on corn cobs and on flax fines. Others come from the industry such as black liquor

(by-product from the paper industry), molasses (by-product from the sugar industry), commercial lignin  
25 (by-product from the wood industry) and the PLA (thermoplastic binder from renewable resources).  
Secondly, two types of aggregates: hemp shiv and corn cob residues (obtained after alkali treatment on  
the corn cob) for their good hygric property, are considered. Then, specimens are produced to verify  
the gluing effect, to qualify the mechanical properties and the hygrothermal performances of developed  
composites. The aim of these characterizations, in link with the objectives in terms of reduction of  
30 the energy needs of buildings and in terms of hygrothermal comfort of users, is to identify the best  
aggregate-binder mixture.

## 2. Materials and methods

### 2.1. Raw materials

#### 2.1.1. Binders

35 Interesting gluing effect is quoted in the case of compressed straw panels, where no additional binder  
is needed to provide a minimum of cohesion. The raw material is just cleaned and compressed between  
two hot plates where it undergoes a hydrothermal treatment at 200°C (as the STRAMIT Process  
[7]). The cohesion of the obtained material is then ensured by the released lignin (between 8 and 17  
%), hemicellulose (between 28 and 33 %) and cellulose (between 33 and 42 %) from wheat straw [8].  
40 Based on this observation, it is possible to use the components contained in the bio-based aggregates to  
formulate a green binder.

Initial work was done to evaluate the ability of hemp shiv to be bonded by wheat straw using similar  
process with hydrothermal treatment and compression. Hemp shiv was mixed with wheat straw chopped  
with a lab blender to obtain bio-based composites. Several compositions were tested; it was shown that  
45 wheat straw ensured a good cohesion to the composite when the dry mix included at least 15 w% of  
chopped wheat straw [9].

Another process is investigated in this study to obtain bio-binder by extraction of soluble components. The extraction process consists in infusing wheat straw in solvent for several hours. Then, wheat straw is pressed in order to collect all the solvent. This solvent is partially evaporated in order to control the concentration of the solution (Figure 1).

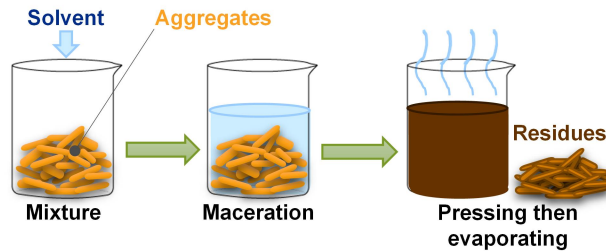


Figure 1: The extraction process on bio-aggregates

Several trials are achieved to identify the optimum conditions. Indeed many factors can affect the efficiency of the extraction process:

- The maceration time;
- The grain size of aggregate;
- The nature of solvent;
- The solvent concentration.

From these trials, the optimum identified conditions are a maceration in alkali solvent during 4 hours at 90°C. The best solvent types and concentrations are deduced.

This process is then applied to several raw materials: hemp shiv and fines, flax shiv and fines, rape straw, wheat straw and corn cobs. These raw materials are supplied by CAVAC, industrial partner of ISOBIO project, and are presented in other paper [10]. Two raw materials allow to have extracts with good gluing properties and a satisfactory extraction yield (over 30 %): corn cobs and flax fines. The weight loss of agro-resources due to the extraction in the alkali solvent, is 39.51 % for the corn cobs and

is 24.27 % for the flax fines. The Van Soest method described in [10], gives the chemical composition including weight loss of the corn cobs and the flax fines before and after extraction (Table 1 and Figure 2). The materials after extraction are called residues, the binders obtained after extraction are named corn cob extract and flax fine extract.

Table 1: Chemical composition of corn cobs and flax fines before and after the alkali-treatment (including weight loss)

Agro-resources	Cellulose (%)	Hemicellulose (%)	Lignin (%)	Solubles (%)	Ash (%)
Corn Cobs	36.78 ± 0.96	38.81 ± 0.72	3.30 ± 0.10	19.30 ± 1.74	0.46 ± 0.01
Corn cob residues	27.10 ± 0.47	13.87 ± 0.86	0.64 ± 0.09	17.53 ± 1.23	0.43 ± 0.07
Flax fines	28.51 ± 0.79	15.80 ± 0.26	18.14 ± 0.28	29.15 ± 0.35	4.20 ± 0.07
Flax fine residues	16.21 ± 1.09	5.83 ± 0.71	7.74 ± 0.47	42.89 ± 3.60	2.92 ± 1.09

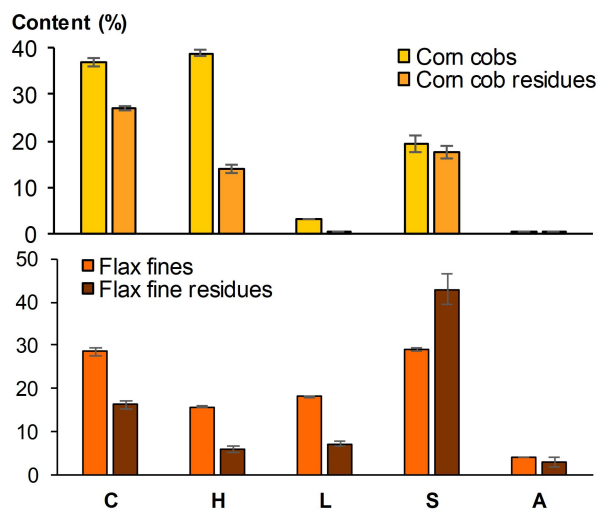


Figure 2: The chemical composition of the corn cobs (up) and flax fines (down) before and after the alkali-treatment (C: Cellulose, H: Hemicellulose, L: Lignin, S: Solubles and A:Ash)

For corn cobs, the alkali treatment leads to substantial removal of cellulose (36.8 % before against 27.1 % after), hemicellulose (38.8 % before against 13.9 % after) and lignin (3.3 % before against 0.7 % after) but only modest dissolution of solubles content (19.3 % before against 17.5 % after) and ash content (0.5 % before against 0.4 % after). For flax fines, the alkali treatment leads to substantial removal of cellulose (28.5 % before against 16.2 % after), hemicellulose (15.8 % before against 5.8 %

after) and lignin (18.1 % before against 7.7 % after), only modest dissolution of ash content (4.2 % before against 2.9 % after) but a significant increase of solubles (29.1 % before against 42.9 % after).

75 These differences can be explained by the weight loss after the treatments. Indeed, the main advantage of alkali treatment is efficient extraction of hemicellulose, lignin and pectin which allows to increase the exposed surface area for the reaction sites for further polymerization. However, this type of treatment has the disadvantage of forming salt and generating degradation if the time of treatment is too long. These degradations can lead to glycosidic bond (O between two aromatic rings in cellulose,  
80 hemicellulose and pectins) break which may change the structure with the repolymerization of released monomer units, the cellulose swelling and its partial decrystallization (Figure 3) [11, 12, 13, 14].

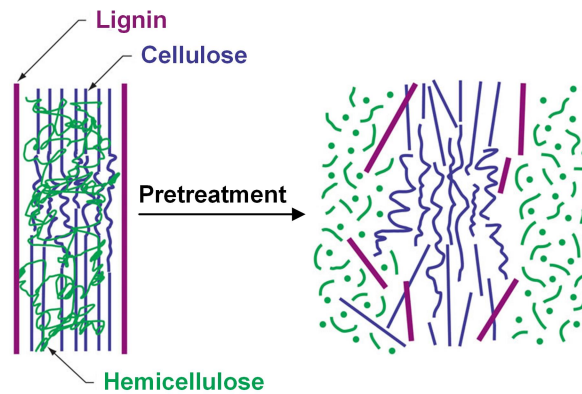


Figure 3: Schematic of alkali-treatment effects on agro-resources [12]

Thus, solutions of alkaline extract from the corn cobs and the flax fines are composed of cellulose, of hemicellulose, of lignin, of solubles and of ash or of their monomer units, repolymerized or not, following the alkali treatment. These components play the role of binder during composite curing (2 hours at  
85 190°C) which allows to initiate repolymerization reactions.

Three other binders are selected as bio-binders coming from the industry: black liquor (waste from the paper industry), molasses (by-product from the sugar industry) and commercial lignin (by-product from the wood industry, Biochoice® powder provided by Domtar).

The last selected binder is a biodegradable thermoplastic from renewable resources: the Poly-Lactic  
90 Acid (PLA provided by Galactic - Belgium). This polymer is characterized by very high mechanical  
properties (flexural strength of 17.8 MPa and compression strength higher than 50 MPa, elastic modulus  
of 3500 MPa) and glass transition temperature around 180°C. PLA is marketed in granular form. To  
be used, it is reduced in chips.

Finally, six types of binders are considered in this study : two green binders which are specifically  
95 developed here and four binders coming from the industry.

### *2.1.2. Aggregates*

Two types of aggregates are considered in this study (Figure 4).

The hemp shiv is a commercial product (Biofibat – CAVAC, France) commonly used to produce  
hemp concrete. Its bulk density is about 100 to 110 kg/m<sup>3</sup>. The average width of aggregates ( $W_{50}$ ) is  
100 2.2 mm and the average length ( $L_{50}$ ) is 8 mm. The maximal width is 5 mm and the maximal length is  
19 mm.

The corn cob is the part of the ear on which kernels grow and is thus, a by-product coming from  
corn cultivation. It is processed to obtain aggregates. The bulk density is about 390 kg/m<sup>3</sup>. The  
average width of aggregates is 3.78 mm and the average length is 5.15 mm. The maximal width is  
105 4.77 mm and the maximal length is 6.47 mm. This aggregate is used to make a green binder with its  
soluble components in the alkali solvent and the corn cob residues obtained are used as aggregates in  
the composite formulations. After the extraction, the bulk density of the corn cob residues is about 365  
kg/m<sup>3</sup>.



Figure 4: Aggregates used to test composite formulations

## 2.2. Composites

### 110 2.2.1. Design of experiment (DOE)

This study **investigates the effect of formulation on multi-physical properties of composites**. Two types of aggregates and six types of binders are tested. To get a large amount of information, screening design is used: Hadamard matrix. This experience design will allow to understand the effects of factors on the composites properties (thermal conductivity and moisture buffer value) [15]. One factor has 2  
 115 levels, for aggregates (hemp shiv or corn cob residues), and one other factor has 7 levels, for binders (without binder, corn cob extract, flax fine extract, black liquor, BioChoice® lignin, Molasses or PLA).

Then, this experimental design is converted in experiment matrix, which is a mathematical entity. It includes as many lines (noted  $n$ ) as formulations and as many columns (noted  $p$ ) as unknown coefficients in the model. This experimental design can be rewritten in the form of the following equation:

$$\{\mathbf{Y}\} = \{\mathbf{B}\}[\mathbf{X}] + \{\mathbf{e}\} \quad (1)$$

120 with:

- $\{\mathbf{Y}\}$ : response vector;
- $[\mathbf{X}]$ : matrix of the model;
- $\{\mathbf{B}\}$ : coefficient vector;

- $\{\mathbf{e}\}$ : vector of the gaps.

125

The mathematical analysis allows to estimate the coefficients  $\{\mathbf{B}\}$  and the residues  $\{\mathbf{e}\}$  by the least squares method. The effects of the factors on the responses are calculated as:

$$\{\mathbf{B}\} = [{}^t\mathbf{X}\mathbf{X}]^{-1} [{}^t\mathbf{X}]\{\mathbf{Y}\} \quad (2)$$

where  $[{}^t\mathbf{X}\mathbf{X}]^{-1}$  is a dispersion matrix and  $[{}^t\mathbf{X}]$  is the transpose of the matrix. Once the  $B_i$  coefficients are determined, they are used in the following equation to predict the responses  $y_i$ .

$$y_i = B_0 + B_1.x_1 + B_2.x_2 + B_3.x_3 + B_4.x_4 + B_5.x_5 + [\dots] + \Delta + \epsilon \quad (3)$$

with:

130

- $y_i$ : response;
- $x_i$ : level of the factor;
- $B_0$ : theoretical average value of the response (constant);
- $B_i$ : effect of the factor;
- $\Delta$ : the lack of fit;

135

- $\epsilon$ : random error.

The robustness of the defined model is tested with two tools: F-test for the significance of the model and the t-test for significance of the coefficients.

The analysis of variance (ANOVA) studies the differences of average between the experimental and theoretical responses. It determines if the defined model is significant or not. The total variation in

140 Y (total sum of squares, SSTO) is divided into two components: the one is the regression equation component (regression sum of squares, SSR) and the other is the residual component (error sum of squares, SSE). The first is tested in comparison with the second. These components are the sum of the squared deviations and their equations are summarized in the following analysis of variance table (Table 2).

Table 2: Standard analysis of variance table

Source of variation	Degrees of freedom	Sum of square	Mean square	Fisher
Regression	$p$	$SSR$	$MSR = \frac{SSR}{p}$	$F^* = \frac{MSR}{MSE}$
Residual error	$n - p - 1$	$SSE$	$MSE = \frac{SSE}{n - p - 1}$	
Total	$n - 1$	$SSTO$		

with:

$$SSR = \sum (y_i - \hat{y}_i)^2 \quad (4)$$

$$SSE = \sum (\hat{y}_i - \bar{y}_i)^2 \quad (5)$$

$$SSTO = SSR + SSE \quad (6)$$

145 where  $y_i$  are the experimental responses,  $\hat{y}_i$  are the theoretical responses and  $\bar{y}_i$  is the average response. Then the  $F^*$  ratio is compared to a critical variable taken in F-table for  $\alpha = 5\%$  (risk). Thus, if  $F^*$  is higher than the considered critical level, the model is considered to be statistically significant.

Another statistical analysis is performed on the coefficients (Table 3).

Table 3: Table of statistical analysis of the coefficients

Coefficient	$\sigma$	$t_{exp}$	Significance
$B_i$	$\sigma_i = \sqrt{MSE \times c_{ii}}$	$t_{exp,i} = \frac{B_i}{\sigma_i}$	$t_{exp} > t_{th}$

with:

- $\sigma_i$ : standard deviation of  $B_i$ ;
- $c_{ii}$ : diagonal term of the level  $i$  of the  $[\mathbf{tXX}]^{-1}$  dispersion matrix.

Then the  $t_{exp}$  is compared to a critical variable from the t-distribution for  $\alpha = 5 \%$  (risk). Thus, if  $t_{exp}$  is higher than  $t_{th}$ , the factor effect is considered to be statistically significant. If a coefficient is considered not relevant, it is possible to eliminate it but its impact on the adjusted determination coefficient  $R_A^2$  will need to be evaluated.

In the presence of several variables, the determination coefficient  $R^2$  is not suitable to compare the descriptive quality of the different models. The use of the adjusted coefficient of determination  $R_A^2$  is required. This coefficient takes into account the number of variables present in the model. Its calculation is given by the equation:

$$R_A^2 = R^2 \times \frac{n-1}{DF} = 1 - \frac{\sum(y_i^2)}{(n-1) \times var(y_i)} \times \frac{n-1}{n-p-1} \quad (7)$$

The closer to 1 the  $R_A^2$  is, the closer to experimental values the calculated values will be [16, 17].

Finally, the interaction graph and the path diagram give the synthetic analysis of the results.

### 2.2.2. Composite production process

Table 4 shows the formulation of the produced composites.

The binder is dissolved in water and then the bio-aggregates are moistened with the solution, except for PLA where PLA chips are mixed with bio-aggregates and the mix is then moistened with water. To ensure a good cohesion, a content of 15 % by weight of dry binder is used. In order to produce three specimens ( $100 \times 100 \times 100 \text{ mm}^3$ ) for each composite, the mix is divided into three equal parts and each part is introduced in one of the three cells of the mold. After, in order to reach an efficient compaction of composite, each part undergoes 5 compression cycles at 0.25 MPa in the mold. At the end

Table 4: Formulation of composites

<b>N°</b>	<b>Aggregates (A)</b>	<b>Binder (B)</b>	<b>B/A ratio</b>
0A	Hemp shiv	Without	0 w%
1	Hemp shiv	Corn cob extract	15 w%
2	Hemp shiv	Flax fine extract	15 w%
3	Hemp shiv	Black liquor	15 w%
4	Hemp shiv	BioChoice® lignin	15 w%
5	Hemp shiv	Molasses	15 w%
6	Hemp shiv	PLA	15 w%
0B	Corn cob residues	Without	0 w%
7	Corn cob residues	Corn cob extract	15 w%
8	Corn cob residues	Flax fine extract	15 w%
9	Corn cob residues	Black liquor	15 w%
10	Corn cob residues	BioChoice® lig	15 w%
11	Corn cob residues	Molasses	15 w%
12	Corn cob residues	PLA	15 w%

170 of the 5 cycles, the specimen remains compacted and the pressure is considered constant at 0.25 MPa. The whole is then placed in an oven at 190°C for 2 hours for thermal curing. The three specimens are demolded after free cooling (Figure 5).

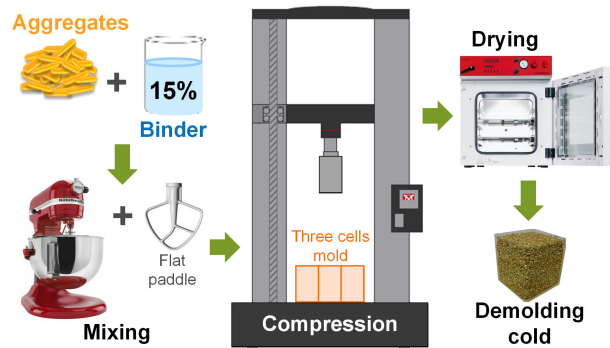


Figure 5: The production of composites

Figure 6 shows the produced composites. The composites n°11 and n°12 show bad cohesion between the binders (molasses and PLA) and the aggregates (corn cob residues). They can't be produced and 175 characterized.



Figure 6: Developed composites

### 2.3. Characterization

#### 2.3.1. Apparent density

The density is calculated from size and weighted of specimens. The three dimensions are measured with an electronic caliper (0.1 mm) and weight with an analytical balance (readability = 0.01 g, reproducibility = 0.01 g, linearity = 0.02 g). Each dimension is the average of four values. This method 180

follows the recommendations of the standard NF EN ISO 12570 [18] which are a measure of volume at close to 1 % and a measure of mass at close to 0.1 % to calculate the apparent density of composites.

### 2.3.2. Skeleton density

The skeleton density  $\rho_s$  is measured with pycnometers [19]. The dry and crumbled composites are placed in pycnometers. Then, they are immersed in toluene and regularly shaken until there is no air remaining. The pycnometers are completely filled with toluene. The successive weighing of pycnometers ( $m_1$ ), pycnometers with dry samples ( $m_2$ ), pycnometers with dry samples and toluene-filled ( $m_3$ ) and water-filled pycnometers ( $m_4$ ) leads to the mass of the samples and their volume (Figure 7). The density of toluene is also measured by pycnometer, filling it with toluene and water. Three pycnometers of about 600 ml are used for each composite.

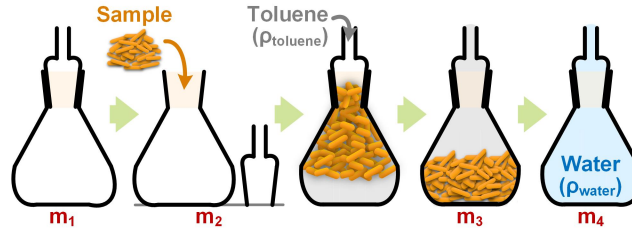


Figure 7: Skeleton density measurement protocol

From the measured weights  $m_1$ ,  $m_2$ ,  $m_3$  and  $m_4$ , the skeleton density  $\rho_s$  of the composites is calculated from the equation (8).

$$\rho_s = \frac{m_{sample}}{V_{sample}} = \frac{m_{sample}}{V_{pycno} - V_{toluene}} = \frac{m_2 - m_1}{\frac{m_4}{\rho_{water}} - \frac{m_3 - m_2}{\rho_{toluene}}} \quad (8)$$

Where the density  $\rho_{toluene}$  corresponds to the density of the toluene and the density  $\rho_{water}$  corresponds to the density of water. The densities  $\rho_{toluene}$  and  $\rho_{water}$  are temperature-dependent.

The total porosity  $n_t$  of composite is the sum of closed and open porosity and intergranular macroporosity. Assuming that the entire porosity has been accessed during pycnometer measurement, the total porosity results in the equation (9).

$$n_t = \frac{\rho_s - \rho_{app}}{\rho_s} \quad (9)$$

with  $\rho_s$  which corresponds to the the skeleton density of the sample and  $\rho_{app}$  to its apparent density.

SEM is used to view the gluing between aggregates and binder. Some aggregates with binder are manually removed from a composite, glued with araldite glue and coated with a layer of palladium (thickness about 30 nm) before the characterization. Scanning electron microscopy (SEM) is performed with a JSM 7100F (Jeol) equipped with Everhart-Thornley secondary electron detector and Schottky field emission.

### 2.3.5. Mechanical characterization

Compressive tests are performed with a Zwick/Roell ProLine testing machine fitted with a 20 kN XForce load cell (load up to 0.02 % of its full capacity and 0.05 % readability) in order to check that the composites are self-bearing. The tests are carried out in displacement with a cross-head speed equal to 0.05 mm.s<sup>-1</sup>. The loading is monotonous (no loading cycles) with testing direction parallel to the compression direction during the production. The samples are placed between two steel plates in order to guarantee a homogeneous displacement and pressure. The load is applied by the displacement of the upper plate. The test is performed on 3 samples for each formulation.

The results of the mechanical tests are analyzed using stress-strain curves, according to the NF EN 826 standard [20]. The stress is assessed by reporting the load to the initial surface of the sample and

the deformation is relative to the initial height of the sample. The origin of the stress-strain curve is adjusted in order to free itself from the contact effects between the plates and the surface of the samples, which is not perfectly flat.

### 2.3.6. Thermal characterization

220 The measurement of thermal conductivity is performed with a transient method: Hot Wire, following the method described by Collet and Pretot [21]. The measurement is realized with the commercial CT Meter device equipped with a five-centimeter long hot wire. The power is 142 mW (n°1 to 4) or 205 mW (n°5 to 10) and the heating time is 120 seconds. [The probe is placed perpendicular to the compression direction during production of composites.](#)

225 Before taking the measurements, the specimens are first dried at 60°C in an oven. Then, the measurements are performed after weight stabilization at 23°C at dry state in desiccator and after weight stabilization at 23°C, 50 %RH in climate chamber. For each formulation, three pairs of specimens (A&B, A&C, and B&C) are measured. The thermal conductivity of a pair is the average of three values with a coefficient of variation lower than 5 %. The thermal conductivity of a composite is the average of the  
230 values obtained for the three pairs (Figure 8).

### 2.3.7. Hygric characterization

The hygric performance is characterized by the measurement of the moisture buffer value (MBV) of composites. This value characterizes the ability of the materials to moderate the variations of indoor humidity in buildings.

235 The moisture buffer value is performed following the Nordtest protocol [22]. After the stabilization of specimens at 23°C, 50 %RH and their sealing on all their surfaces except one ([the one that has been compressed during the production of composites](#)), specimens are exposed for 8 hours at 75 %RH and for 16 hours at 33 %RH during 5 days in a climate chamber (Vötsch VC4060). The specimens are regularly

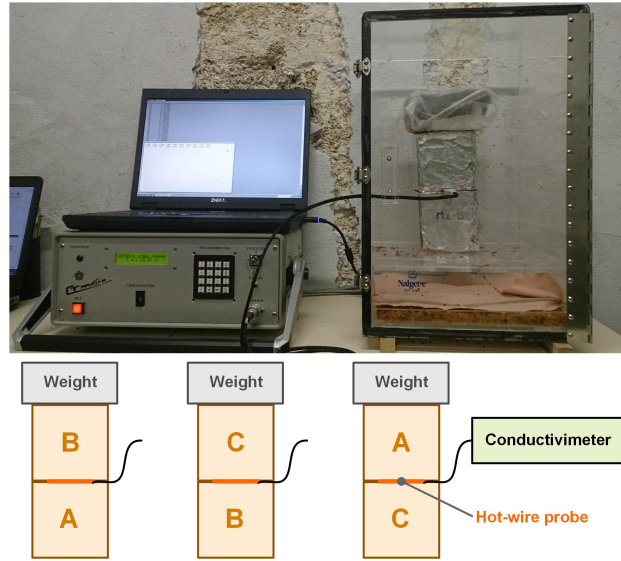


Figure 8: Experimental device for the measurement of thermal conductivity

weighed: five times during the absorption period and two times during the desorption one. The air  
 240 velocity in the climate chamber is consistent with the recommendations of the Nordtest protocol (lower  
 than 0.15 m/s [22]). Then, the moisture buffer value is determined according to the following equation:

$$MBV = \frac{\Delta m}{A \cdot (RH_{high} - RH_{low})} \quad (10)$$

Where MBV is the moisture buffer value (g/(m<sup>2</sup>.%RH)),  $\Delta m$  is the moisture uptake/release during  
 the period (g), A is the open surface area (m<sup>2</sup>),  $RH_{high/low}$  is the high/low relative humidity level (%).

For each formulation, the MBV is the average of the values obtained for the three specimens.

### 245 3. Results

#### 3.1. Apparent and skeleton densities and total porosity

Except for composite n°6, the composites based on hemp shiv have very close densities ranging from  
 177 to 191 kg.m<sup>3</sup> at dry state except the hemp shiv with PLA composite (n°6) which has the highest  
 density (273 kg/m<sup>3</sup>). The composites based on corn cob residues have a density much higher than  
 250 composites based on hemp shiv, due to a much higher aggregate density. The three composites, with

the aggregate extracts and black liquor, have very close densities ranging from 520 to 557 kg/m<sup>3</sup> at dry state. The composite with the lignin has the lowest density (457 kg/m<sup>3</sup> at dry state) of the composites based on corn cob residues. The increase in apparent density between the dry state and the state at (23°C; 50 %RH) ranges from 2.09 % (for the one made with hemp shiv and PLA) to 7.52 % (for the one made with corn cob residues and flax fine extract).

The skeleton density of composites ranges from 1124.6 to 1211.0 kg/m<sup>3</sup> for hemp shiv composites and from 1238.8 to 1310.0 kg/m<sup>3</sup> for corn cob residues composites. The highest values of corn cob residues composites are due to higher skeleton density of aggregate (about 1350 versus 1550 kg/m<sup>3</sup>). The variation of skeleton density with binder shows the same trend for hemp shiv composites and corn cob residues composites. However, it does not vary only with the proportion of each component due to chemical reaction and volatilization during the production of composites.

The composites based on hemp shiv have very close total porosities ranging from 84.2 % to 87.5 % except the one made with PLA. Indeed, it has the lowest total porosity (77.5 %) of the composites made with hemp shiv. However, the composites made with corn cob residues have lower total porosity than the composites made with hemp shiv. Indeed, they have very close porosities ranging from 60.0 % to 65.5 %.

Table 5: Apparent density at (23°C, 50%RH) and (23°C, dry), skeleton density and total porosity of composites: average value and standard deviation

Composites	1	2	3	4	5	6	7	8	9	10
$\rho_{23^{\circ}C-50\%RH}$ (kg/m <sup>3</sup> )	177.7 ± 2.4	179.6 ± 5.7	191.4 ± 0.9	179.0 ± 1.3	187.4 ± 1.4	272.9 ± 18.9	519.9 ± 9.8	556.9 ± 9.7	527.0 ± 5.4	457.3 ± 15.3
$\rho_{23^{\circ}C-dry}$ (kg/m <sup>3</sup> )	167.0 ± 2.1	168.8 ± 5.3	180.7 ± 0.9	170.9 ± 1.1	177.4 ± 1.1	267.2 ± 19.0	481.4 ± 8.6	515.0 ± 7.8	488.4 ± 4.7	427.0 ± 14.0
$\rho_s$ (kg/m <sup>3</sup> )	1130.9 ± 7.3	1178.0 ± 12.5	1211.0 ± 7.2	1150.1 ± 2.4	1124.6 ± 16.9	1186.9 ± 57.7	1249.8 ± 1.4	1286.7 ± 9.8	1310.0 ± 1.4	1238.8 ± 6.4
$n_{tot}$	87.5%	85.7%	85.1%	85.1%	84.2%	77.5%	61.5%	60.0%	62.7%	65.5%

### 3.2. Surface Morphology by Scanning Electron Microscopy

Figure 9 presents SEM micrographs at the interface between the aggregates and the binder. For all composites, SEM analysis evidences good adhesion at the interface showing several hemp shiv well coated and glued together. There are micro-structural differences at the interface between the aggregates and the different types of binders.

The surface of composites n°1 and 2 and 3 (Figures 9.a to 9.d) are similar. The binders lead to a grain deposit on the hemp shiv.

For composite n°4 (Figure 9.e), the hemp shiv are well coated with lignin in some places. The lignin coats the hemp shiv with a more or less thin smooth film depending on the location. Thus, the adhesion between aggregates and binder is good but the increased thickness of the binder may seal the hemp shiv pores in some places.

For composite n°5 (Figure 9.f), the hemp shiv are well coated with molasses. The molasses coat the hemp shiv with a thin rough film.

For composite n°6 (Figure 9.g), the hemp shiv are well coated with PLA in some places. A few large spots of PLA are visible between the hemp shiv so, the PLA coats the hemp shiv with a thick smooth film. Thus, the adhesion between aggregates and binder is good but the thickness of the binder seals the hemp shiv pores and fills the inter-particular space. Indeed, the total porosity is 77.5 % while it is around 85.5 % for other composites made with hemp shiv.

The surface of composites n°7 and 8 (Figures 9.h to 9.j) are similar but different from composites made with hemp shiv for a same binder. It can be explained by the difference in the composition of agro-resources. Indeed, the corn cob residues have been previously treated with an alkaline solution at 90°C. Thus, their surface is more reactive [12, 14] than that of hemp shiv for a same binder. The corn cob residues are coated with a thin smooth layer in some areas but several fracture zones are visible above. More, the composite surfaces include sodium silicate crystals for composites n°7 and 8. A similar

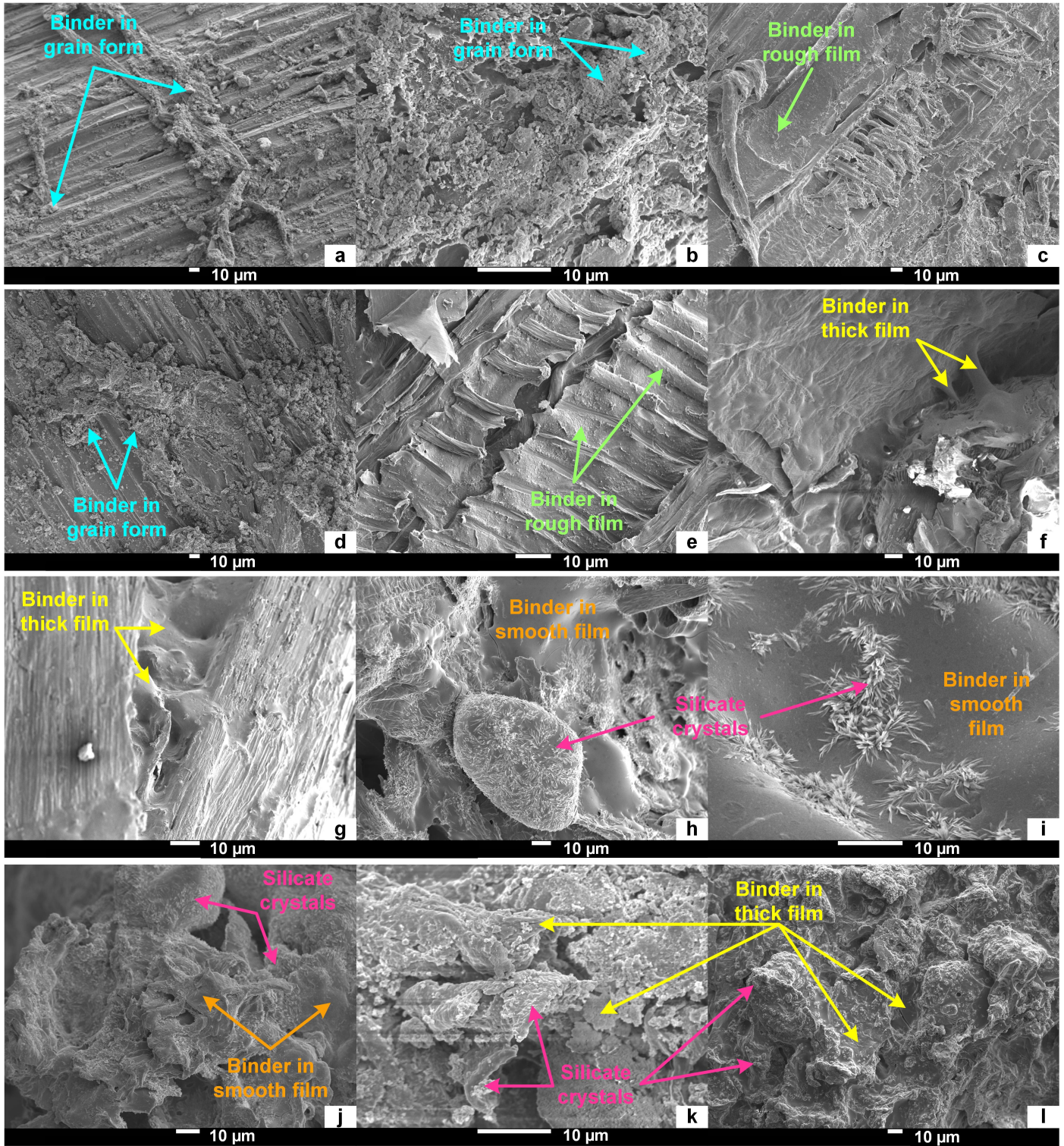


Figure 9: SEM micrographs at the interface between the aggregates and the binder: (a) and (b) composite n°1, (c) composite n°2, (d) composite n°3, (e) composite n°4, (f) composite n°5, (g) composite n°6, (h) and (i) composite n°7, (j) composite n°8, (k) composite n°9 and (l) composite n°10

surface has been observed by El Hajj et al. for their composites made with flax shiv and proteinic binder [23].

For composite n°9 (Figure 9.k), the corn cob residues are well coated with black liquor. The black liquor coats the corn cob residues with a thick rough film. The roughness probably corresponds to mineral salts containing silicates. The adhesion between the corn cob residues and the black liquor seems to be less good than with the extracts.

For composite n°10 (Figure 9.l), the corn cob residues are well coated with lignin. The lignin coats the corn cob residues with a thick rough film which includes several fracture zones. The roughness probably corresponds to mineral salts containing silicates.

### 3.3. Mechanical characterization

Two types of strain-stress curve are obtained.

Curves with a continuous increase in the stress versus strain correspond to compacting behavior (Figure 10.a). For such behavior, the mechanical performance is given by the compressive strength  $\sigma_{10\%}$  obtained for longitudinal strain  $\epsilon = 10 \%$  (Figure 10.a) [20]. Such curves are obtained for hemp shiv composites and corn cob residues composites with extract binders.

Curves with a peak in the stress-strain curve correspond to ductile behavior (Figure 10.b). For such behavior, the mechanical performance is given by the maximal compressive strength  $\sigma_m$  obtained for deformations  $\epsilon_m$  under 10 % (Figure 10.b) [20]. Such curves are obtained for corn cob residues composites with black liquor and BioChoice® lignin.

This behavior difference is mainly explained by the shape of the aggregates (rectangular for hemp shiv and ovoid for corn cob residues) as well as the total porosity of the composites (about 84.2 % for those made with hemp shiv compared to about 62.4 % for those made with corn cob residues).

The mechanical properties of composites are presented in Figure 11 and Table 6. Experimental values

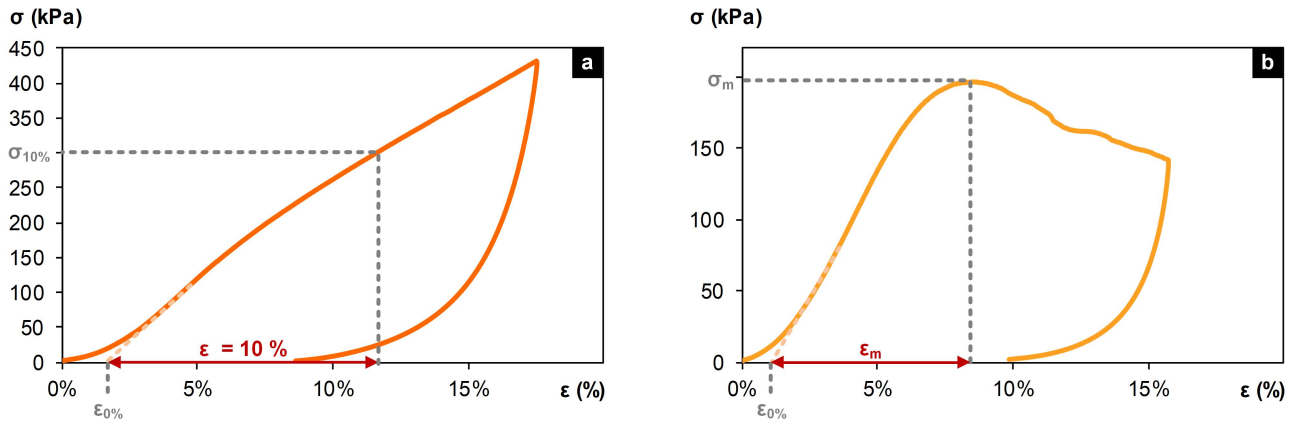


Figure 10: Strain-stress curve for composites 4.b (a) and 9.b (b)

are closer to each other formulation for the composites made with the hemp shiv than those made with  
 315 the corn cob residues. As shown on Figure 11, the compressive strength for the composites made with  
 the hemp shiv and extracts is around 239 kPa whereas the other composites made with the hemp shiv  
 have a better compressive strength due to a better adhesion between the hemp shiv and the binders  
 (range from 227 to 421 kPa). The composite made with hemp shiv and PLA has the highest compressive  
 strength of composites made with hemp shiv. Compressive strength at 10 % deformation, varies between  
 320 492 and 696 kPa for the two specimens made with corn cob residues and extract. Composites n°7 have  
 the highest compression strength. Thus, the corn cob residues have a good adhesion with the extracts  
 (corn cob extract and flax fine extract) although it is better with the corn cob extract. However, the  
 corn cob residues have a poor adhesion with the other binders (black liquor and BioChoice® lignin)  
 because the maximal compressive strengths are 202 and 32 kPa respectively for a deformation lower  
 325 than 7.4 %.

The compressive strength at 10 % deformation of composites is higher than 225 kPa **except composites n°9 and n°10 (corn cob residues/black liquor and corn cob residues/BioChoice® lignin)**. According to the composite densities, for stress corresponding to 3 meters in height, the obtained deformations ( $\epsilon_{h=3m}$ ) are lower than 0.50 %. So, the mechanical properties are sufficient for an application as insulation

330 panels without risk of compaction.

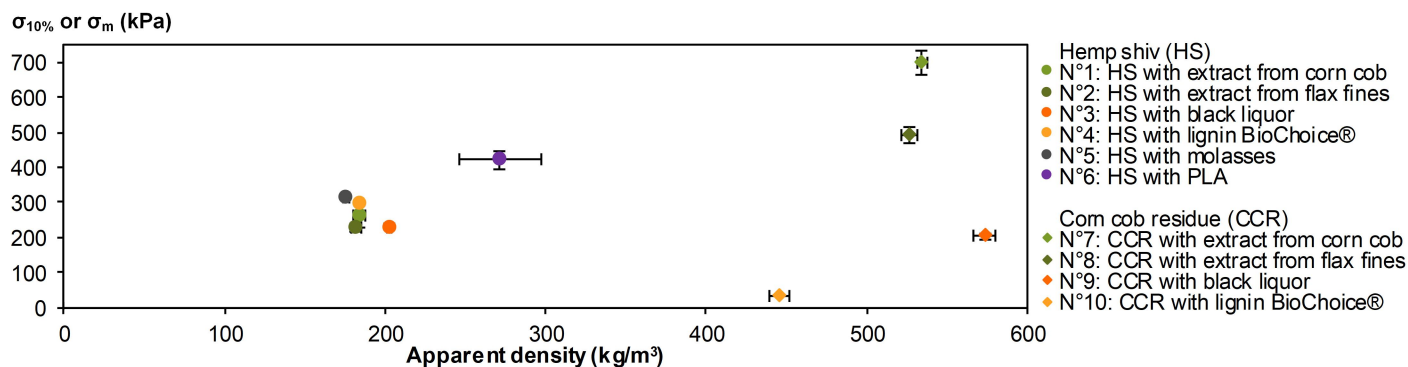


Figure 11: Stress at 10 % deformation or maximal stress versus apparent density at 23°C and 50 %RH of composites

Table 6: Stress at 10 % deformation or maximal stress for each composites

Composites	1	2	3	4	5	6	7	8	9	10
$\rho_{23^{\circ}C-50\%RH}$ (kg/m <sup>3</sup> )	184.2 ± 4.1	181.9 ± 3.1	203.2 ± 1.1	184.4 ± 0.7	175.6 ± 2.1	271.7 ± 26.0	534.5 ± 3.5	526.8 ± 4.8	573.4 ± 6.7	445.9 ± 6.5
$\sigma_{10\%}$ (kPa)	259.7 ± 34.2	227.5 ± 9.9	230.0 ± 6.5	297.3 ± 4.2	313.7 ± 2.4	420.8 ± 25.7	695.7 ± 42.7	491.8 ± 47.8	-	-
$\sigma_m$ (kPa)	-	-	-	-	-	-	-	-	202.3 ± 32.7	31.9 ± 7.4
$\epsilon_m$ (%)	-	-	-	-	-	-	-	-	7.28	2.95
$\epsilon_{h=3m}$ (%)	0.20	0.22	0.22	0.16	0.14	0.13	0.36	0.47	0.47	2.95

335 Compared with compressive strength at 10 % deformation obtained in the literature, these values are lower. Indeed, Nguyen et al [24], who studied composites made with bamboo fibers and bio-glues have obtained better results as they range from 2700 to 14200 kPa (densities from 311 to 538 kg/m<sup>3</sup>). Beside, the hemp-starch composites developed by Bourdot et al [25] have similar mechanical properties

340 except the one made with corn cob residues and corn cob extract which have better properties (around 700 kPa for density around 125 kg/m<sup>3</sup> at 10 % deformation). Compared with maximal compressive strength obtained by Ratiarisoa et al [26] for the composites made with residues of lavender and mineral pozzolanic binder this value (220 kPa for density around 620 kg/m<sup>3</sup> at dry state) is slightly better than this obtained for the composites made with corn cob residues and black liquor (203 kPa).

### 3.4. Thermal characterization

To validate thermal conductivity measurement, an infrared thermography picture is taken on each specimen immediately after the measurement. For all specimens, all the volume influenced by the probe is included in the specimen volume, as shown as examples on Figure 12 for composites n°5 (left) and n°8 (right). The thermal footprint shows that ①: the heat flow remains in the sample during the measurement and that ②: the probe volume is representative of the material. Thus, the measurements are representative of the studied materials.

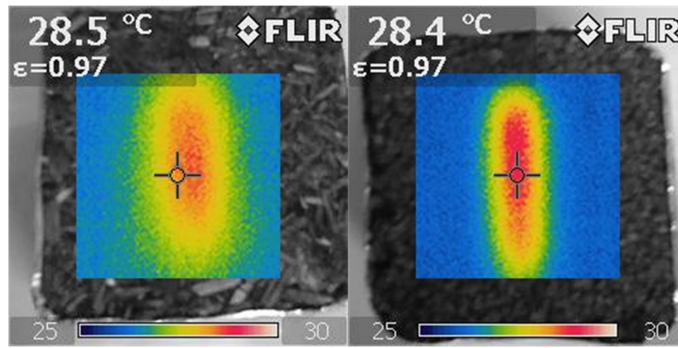


Figure 12: Infrared thermography pictures of specimens 5 (on the left) and 8 (on the right) immediately after the thermal conductivity measurement

Table 7 and Figure 13 show the thermal conductivity for the different formulations developed in this study.

Table 7: Thermal conductivity of composites (mW/(m.K)) versus apparent density at (23°C, 50%RH) and at (23°C, dry)

Composites	1	2	3	4	5	6	7	8	9	10
$\rho_{23^{\circ}C-50\%RH}$ (kg/m <sup>3</sup> )	176.4 ± 2.1	178.5 ± 5.6	190.4 ± 1.0	178.1 ± 1.3	186.1 ± 1.1	272.7 ± 19.3	513.0 ± 8.7	547.5 ± 7.9	521.5 ± 5.4	455.7 ± 17.0
$\lambda_{23^{\circ}C-50\%RH}$ (mW/(m.K))	78.5 ± 1.3	78.1 ± 1.8	78.2 ± 3.3	75.6 ± 1.8	77.8 ± 1.6	81.2 ± 4.0	156.9 ± 5.3	171.6 ± 4.5	157.7 ± 5.1	143.5 ± 2.8
$\rho_{23^{\circ}C-dry}$ (kg/m <sup>3</sup> )	167.0 ± 2.1	168.8 ± 5.3	180.7 ± 0.9	170.9 ± 1.2	177.4 ± 1.1	267.2 ± 19.0	481.4 ± 8.6	515.0 ± 7.9	488.4 ± 4.7	427.0 ± 14.0
$\lambda_{23^{\circ}C-dry}$ (mW/(m.K))	70.8 ± 0.9	70.2 ± 1.2	71.1 ± 1.5	67.5 ± 1.3	70.5 ± 0.8	78.6 ± 1.7	140.3 ± 4.1	147.9 ± 4.7	136.5 ± 4.8	128.4 ± 4.7

At dry state, the thermal conductivity of developed composites ranges from 67.5 to 78.6 mW/(m.K)

for hemp shiv composites and from 128.4 and 147.9 mW/(m.K) for corn cob residues composites. The lowest values of hemp shiv composites are due to lower thermal conductivity of aggregate (53.5 versus 85.1 mW/(m.K)).

The composite with the PLA has a thermal conductivity slightly higher than the others made with the hemp shiv. The composite with the BioChoice® lignin has a thermal conductivity slightly lower than the others made with the corn cob residues.

As shown on Figure 13.a, the thermal conductivity of the composites increases linearly with density. The correlation coefficient of the fitting curve is very close to 1. The slope of the regression curve for the composites (yellow curve), is more important than the slope of the regression curve for the aggregates (green curve corresponding to bio-aggregates studied in [10]). Thus, the thermal conductivity increases more quickly with the apparent density in the case of the composites.

As shown on Figure 13.b, the thermal conductivity of the composites is higher at (23°C; 50 %RH) than at (23°C; dry). The regression lines of the thermal conductivity versus the apparent density at dry state and at 23°C, 50 %RH are almost parallel but the intercept of the regression line for the composites at dry state (yellow curve), is lower than the intercept of the regression line for the composites at 23°C, 50 %RH (orange curve). Indeed, the apparent density of the composites increases with the increased ambient humidity (including an increase in water content), resulting in the increase in the thermal conductivity.

To obtain additional information, the thermal conductivity values obtained at dry state, are exploited through the design of experiment. Following the F-test (analysis of variance), the model with 6 coefficients is significant and has the best adjusted determination coefficient ( $R_a^2 = 0.9319$ ) and determination coefficient ( $R^2 = 0.9437$ ). Thus, the equation to predict the thermal conductivity at dry state is the following:

- N°0A: Hemp shiv (HS)
- N°1: HS with extract from corn cob
- N°2: HS with extract from flax fines
- N°3: HS with black liquor
- N°4: HS with lignin BioChoice®
- N°5: HS with molasses
- N°6: HS with PLA
- N°0B: Corn cob residue (CCR)
- ◆ N°7: CCR with extract from corn cob
- ◆ N°8: CCR with extract from flax fines
- ◆ N°9: CCR with black liquor
- ◆ N°10: CCR with lignin BioChoice®

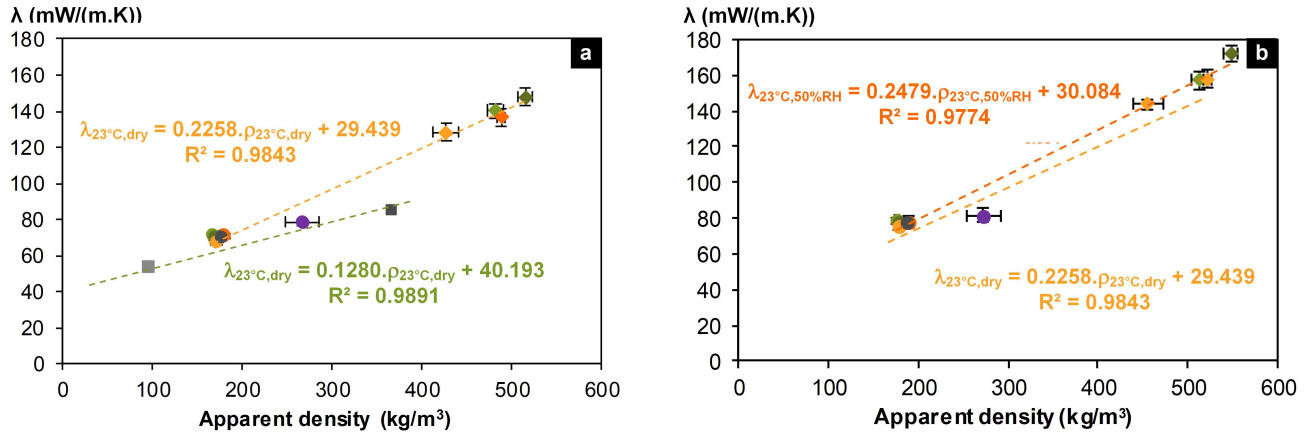


Figure 13: Thermal conductivity of composites versus their apparent density : (a) Comparison between the composites and the aggregates [10] at (23°C; dry) and (b) Comparison between the thermal conductivity values of the composites at (23°C; dry) and at (23°C; 50 %RH).

$$\lambda_i = 38.56 + 60.97 \times x_1 + 36.35 \times x_2 + 40.13 \times x_3 + 34.75 \times x_4 + 28.88 \times x_5 \quad (11)$$

Figure 14 shows the interactions between the aggregates and the binders. The slope of the lines for the composites, whatever the binder, is more important than the slope of the line in the case of the bulk. The interaction between the hemp shiv and the binders is the same except for the PLA where the interaction is more important. The lines of the corn cob extract and the black liquor are confused. Their impact is the same on the thermal conductivity for these two aggregates. The interaction between the corn cob residues and the binders is not the same. Indeed, it is more important for the flax fine extract and less important for the BioChoice® lignin.

For an identical production process, Figure 15 shows that thermal conductivity increases when the hemp shiv are replaced by the corn cob residues (B1 coefficient) and when the bulk is converted into composites (coefficients B2, B3, B4 and B5). Indeed, the density of the composites increases with the use

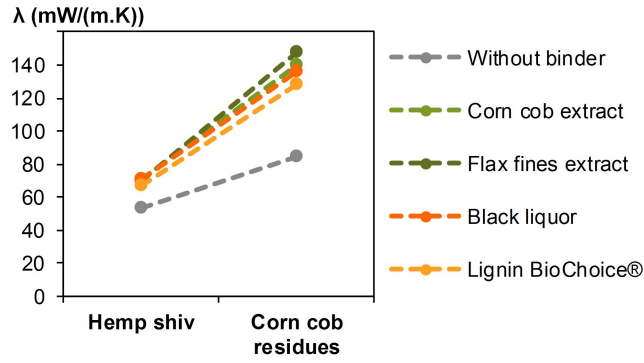


Figure 14: Interaction graph for the thermal conductivity at dry state (mW/(m.K))

of corn cob residues as aggregates. The binder with the least important impact is the lignin (coefficient B5). The corn cob extract (coefficient B2) and the black liquor (coefficient B4) both have high impact on the thermal conductivity (nearly the same). The path diagram gives the flax fine extract the highest impact. However, the impact of flax fine extract is much higher on corn cob composites than on hemp shiv composites. Indeed, the impact induced by flax fine extract is not only due to the type of binder but also to its effect on composite apparent density.

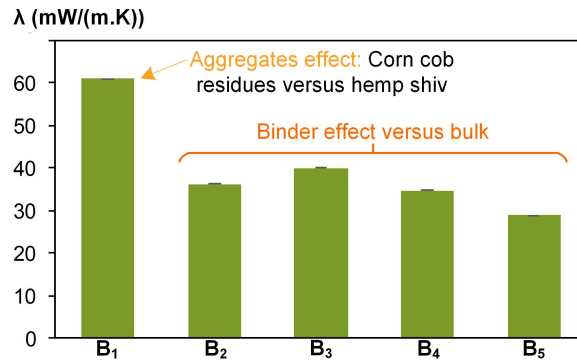


Figure 15: Path diagram for the thermal conductivity at dry state (mW/(m.K))

Compared with other bio-based composites, the hemp composites have higher thermal conductivity than commercial soft hemp insulation materials in the UK. Indeed, the thermal conductivity of the commercial products ranges from 38 to 43 mW/(m.K) for density around 50 kg/m<sup>3</sup> at dry state [27]. Thus, this difference is mainly explained by the lowest density of the composites found in literature.

However, hemp-starch composites have a similar thermal conductivity. Indeed, the thermal conductivity  
395 of hemp-starch ranges from 48 to 74 mW/(m.K) for density around 125 kg/m<sup>3</sup> at dry state [25].

The corn cob residues composites have higher thermal conductivity than the composites made with  
bamboo fibers and bio-glues and similar to the composites made with residues of lavender and mineral  
pozzolanic binder. Indeed, the thermal conductivity ranges from 55 for low density (311 kg/m<sup>3</sup>) to  
88 mW/(m.K) for high density (538 kg/m<sup>3</sup>) at 25°C and 57 %RH for the composites made with bamboo  
400 fibers and bio-glues [24] whereas the thermal conductivity ranges from 142 to 162 mW/(m.K) for density  
around 620 kg/m<sup>3</sup> at dry state for the composites made with residues of lavender and mineral pozzolanic  
binder [26].

### 3.5. Hygric characterization

Figure 16 shows the ambient relative humidity and temperature in the climate chamber during  
405 the test. The average value of relative humidity is slightly lower than 75 % during absorption (about  
71.4 %) and slightly higher than 33 % during desorption (about 35.5 %) due to the fact that the door of  
the climate chamber is regularly opened to weigh specimens (peak on the curve).

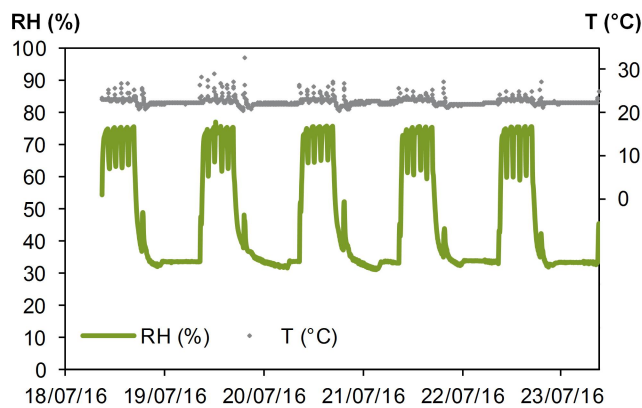


Figure 16: Monitored relative humidity and temperature in the climate chamber during MBV test

An example of the moisture uptake and release of a specimen is shown by Figure 17. The change in  
mass is lower than 5 % for cycles 3 to 5 for all composites. So, the moisture buffer value is determined

410 from cycles 3 to 5.

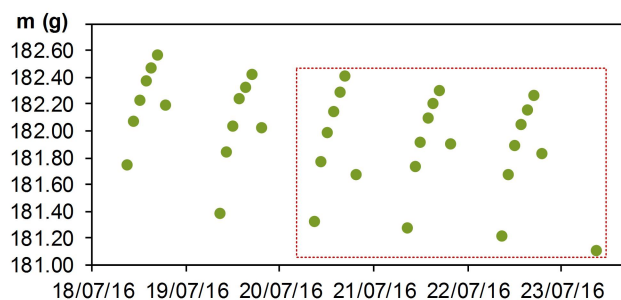


Figure 17: Moisture uptake and release for sample n°1-A

Table 8, Figures 18 and 19 summarize the moisture buffer values obtained in absorption, desorption and in average. The standard deviations are low, leading to coefficients of variation lower than 4.5 %.

The average MBV ranges from 1.86 to 5.08  $\text{g}/(\text{m}^2 \cdot \%RH)$ . According the Nordtest classification [22], only composite n°6 is good hygric regulator ( $1 < MBV < 2 \text{ g}/(\text{m}^2 \cdot \%RH)$ ). The others composites are  
415 all excellent hygric regulators ( $MBV > 2 \text{ g}/(\text{m}^2 \cdot \%RH)$ ).

As shown on Figures 18 and 19, the composites made with corn cob residues have a better MBV than the composites made with hemp shiv for a same binder. That makes sense because in bulk, the corn cob residues already have a better MBV than the hemp shiv.

The composites made from similar binders (corn cob extract, flax fine extract and black liquor)  
420 and hemp shiv, have close MBV around  $3.14 \text{ g}/(\text{m}^2 \cdot \%RH)$ . These composites have the best MBV of composites made with hemp shiv probably due to a grain deposit of the binder which increases the specific surface area available for moisture adsorption. Composite n°6, which has the lowest MBV ( $1.86 \text{ g}/(\text{m}^2 \cdot \%RH)$ ), is made with hemp shiv and PLA. This is probably due to the fact that PLA reduces the accessible porosity. The others composites made from hemp shiv have a MBV slightly  
425 higher around  $2.05 \text{ g}/(\text{m}^2 \cdot \%RH)$ . The composite made from similar binders (corn cob extract, flax fine extract and black liquor) and corn cob residues also have close MBV, around  $4.90 \text{ g}/(\text{m}^2 \cdot \%RH)$ .

Thus, the MBV is impacted by the type of aggregate and binder, not only by bulk density.

Table 8: Moisture Buffer Value of composites in absorption, desorption and average: average value and standard deviation

Composites	1	2	3	4	5	6	7	8	9	10
$MBV_{abs.}$	3.05	3.10	2.96	2.00	2.02	1.84	4.70	4.69	4.98	3.89
$g/(m^2.\%RH)$	$\pm 0.11$	$\pm 0.11$	$\pm 0.14$	$\pm 0.06$	$\pm 0.05$	$\pm 0.07$	$\pm 0.07$	$\pm 0.06$	$\pm 0.21$	$\pm 0.04$
$MBV_{des.}$	3.19	3.23	3.09	1.89	2.09	1.89	4.88	4.95	5.19	4.10
$g/(m^2.\%RH)$	$\pm 0.10$	$\pm 0.13$	$\pm 0.14$	$\pm 0.06$	$\pm 0.04$	$\pm 0.09$	$\pm 0.10$	$\pm 0.07$	$\pm 0.16$	$\pm 0.07$
$MBV_{av.}$	3.12	3.16	3.12	2.05	2.05	1.86	4.79	4.82	5.08	3.99
$g/(m^2.\%RH)$	$\pm 0.09$	$\pm 0.11$	$\pm 0.14$	$\pm 0.06$	$\pm 0.04$	$\pm 0.07$	$\pm 0.08$	$\pm 0.06$	$\pm 0.18$	$\pm 0.05$

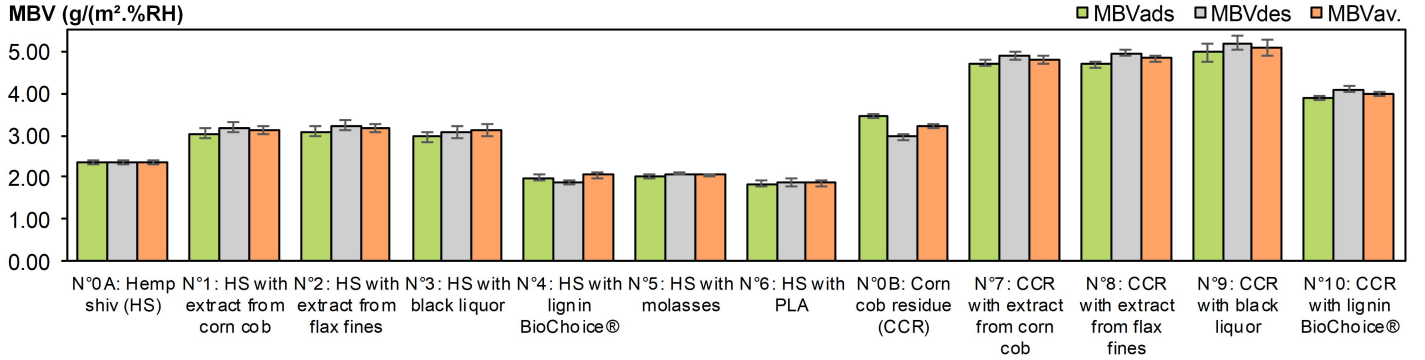


Figure 18: Moisture buffer value ( $g/(m^2.\%RH)$ ) versus composites

To obtain additional information, the results are exploited through the design of experiment.

Following the F-test (analysis of variance), the model with 8 coefficients is significant and has the  
430 best adjusted determination coefficient ( $R_a^2 = 0.9886$ ) and determination coefficient ( $R^2 = 0.9909$ ) which  
are close to 1. Thus, the equation to predict the moisture buffer value is the following:

$$MBV_i = 2.38 + 0.86 \times x_1 + 1.16 \times x_2 + 1.20 \times x_3 + 1.26 \times x_4 + 0.23 \times x_5 - 0.30 \times x_6 - 0.48 \times x_7 \quad (12)$$

Figure 20 shows the interactions between the aggregates and the binders. The lines of the two  
extracts are confused. Their impact is the same on the MBV for these two aggregates. The slope of the  
lines for the black liquor and the BioChoice® lignin are the same. However, the interaction between  
435 the black liquor and the aggregates is better than the one of the BioChoice® lignin. The interaction  
between the hemp shiv and the binders are the same for the extract binders and the black liquor. The

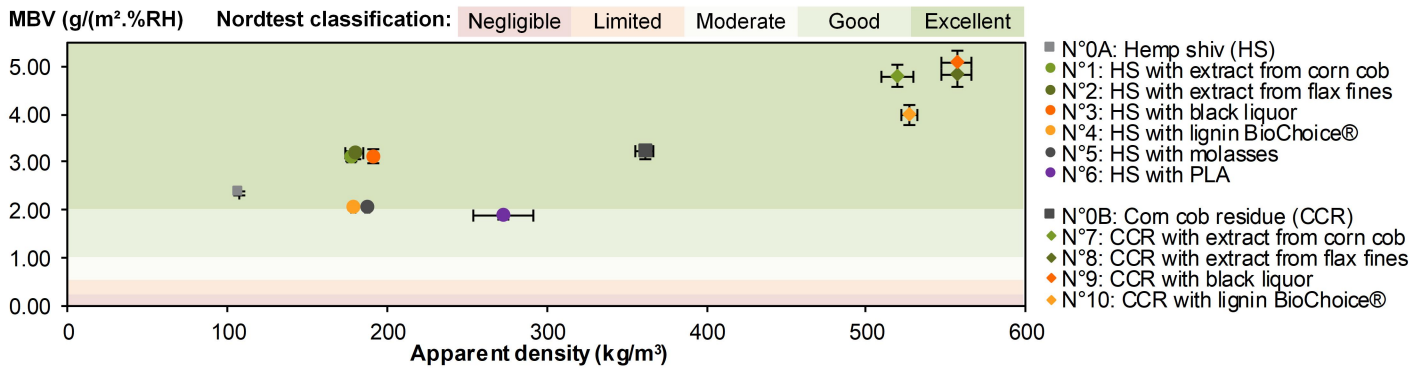


Figure 19: Average moisture buffer value of composites ( $\text{g}/(\text{m}^2.\%RH)$ ) versus apparent density

interaction between the hemp shiv and the other binders is less important as the synergy is negative. The interaction between the corn cob residues and the binders is not the same. Indeed, it is more important for the black liquor and less important for the BioChoice® lignin.

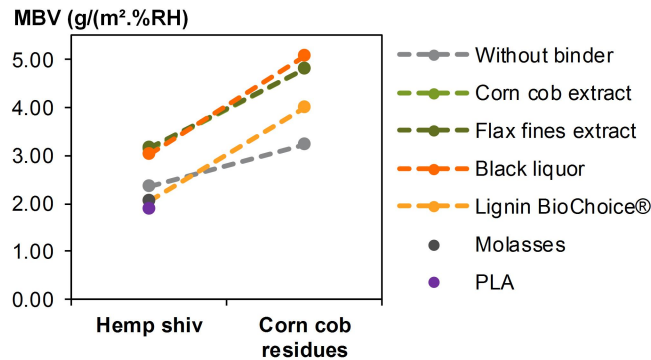


Figure 20: Interaction graph for the moisture buffer value ( $\text{g}/(\text{m}^2.\%RH)$ )

440 Figure 21 shows that MBV increases when the hemp shiv are replaced by the corn cob residues (coefficient B1) and when the bulk is converted into composites (coefficients B2, B3, B4 and B5). For the coefficients B6 and B7, when the bulk is converted into composites, the MBV decreases. These binders seal the pores of agro-resources because the shiv are coated with a thick film. The binder which has the most important impact on the increase of the MBV is the black liquor (coefficient B4). The  
 445 binder with the least important positive impact is the BioChoice® lignin (coefficient B5). The corn cob extract (coefficient B2) and the flax fine extract (coefficient B3) have nearly the same impact on the

MBV. This impact is somewhat less important than the one of black liquor.

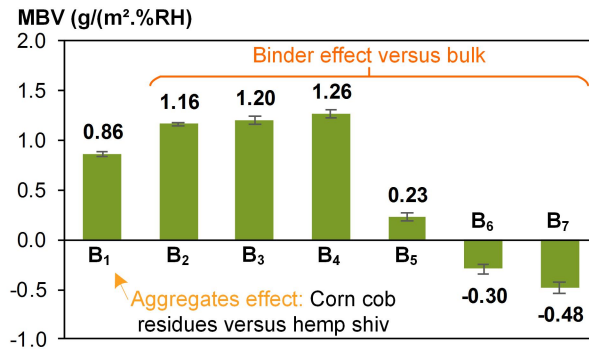


Figure 21: Path diagram for the moisture buffer value ( $\text{g}/(\text{m}^2.\%RH)$ )

Compared with other bio-based composites, the hemp composites are in the average of the MBV. For commercial hemp insulation materials in the UK, the MBV ranges from 1.5 to 2.7  $\text{g}/(\text{m}^2.\%RH)$  [27], while for hemp-starch, the MBV ranges from 2.4 to 3.4  $\text{g}/(\text{m}^2.\%RH)$  [28].

Compared with other bio-based composites, the corn cob residues composites have the highest MBV. For the composites made with residues of lavender and mineral pozzolanic binder, the MBV ranges from 3.5 to 3.9  $\text{g}/(\text{m}^2.\%RH)$  [26], while the composites made with bamboo fibers and bio-glues, the MBV ranges from 2.5 to 3.5  $\text{g}/(\text{m}^2.\%RH)$  [24].

#### 4. Conclusion

This study shows that it is possible to produce fully bio-based composites. Indeed, the use of these combinations of binders and aggregates is very interesting from the environmental perspective because local agriculture is given priority, waste and by-products are used in the production of these binders where none additive is used.

Two green binders produced from alkaline extraction carried out on corn cobs and flax fines, have been developed throughout this work. This process allows to extract some cellulose, hemicellulose, lignin and pectin content, repolymerized or not, with a good reactivity under heating. So, these extracts are

used as binder. During the production of composites, the composite curing step allows to initiate the repolymerization of components contained in the agro-resources extracts.

465 With a zero waste perspective, the corn cob residues that left after the alkali extraction are used as aggregates in this study. They have the advantage to have more important specific surface areas (for further polymerization) than the untreated corn cobs. Their cohesion with binder should be better and so, their mechanical properties improved. The performances of composites made with these aggregates have been compared with those of composites made with hemp shiv.

470 The density of developed composites ranges from 177 to 273 kg/m<sup>3</sup> with hemp shiv as aggregates, and ranges from 457 to 557 kg/m<sup>3</sup> with corn cob residues as aggregates. Their mechanical performances are sufficient to be used as self bearing materials. The thermal conductivity ranges from 67.5 to 147.9 mW/(m.K). It is mainly dependent on density but it is also slightly impacted by the type of binder. Thus, the composites made with hemp shiv have a lower thermal conductivity than the ones made with  
475 the corn cob residues. The composites are all excellent hygric regulators ( $MBV > 2 \text{ g}/(\text{m}^2 \cdot \%RH)$ ) except the composite made with PLA, which is only a good hydric regulator. For a same binder, the composites made with corn cob residues have a better MBV than the composites made with hemp shiv. More, the use of the molasses and the PLA decreases the MBV because these binders seem to seal the pores of agro-resources.

480 Finally, the production of a two-layer thermal insulating panel would be ideal. Indeed, the composites made with hemp shiv can be used for distributed insulation because they have a low thermal conductivity. Moreover, it may be even lower if the density of the composites is decreased. It is interesting to add a second layer made of corn cob residues and extracts from agro-resources, one centimeter thick, for its excellent ability to moderate the variations of the relative humidity in the surrounding air. Thus,  
485 further research is still required to qualify the hygrothermal properties of a such multi layer system in real condition.

## Acknowledgments

This project has received funding from the European Union's Horizon 2020 research and innovation program under grant agreement No. 636835 – The authors would like to thank them.

490 CAVAC, industrial partner of the ISOBIO project, is gratefully acknowledged by the authors for providing raw materials.

Thanks are due to Tony Hautecoeur for his participation in the completion of this work.

Loïc Joanny and Francis Gouttefangeas are acknowledged for SEM images performed at CMEBA (ScanMAT, University of Rennes) which received a financial support from the Région Bretagne and  
495 European Union (CPER-FEDER 2007-2014).

Thanks are due to Étienne Labussière (Van Soest analysis) and Yann Lecieux (Mechanical tests).

Thanks are also due to Céline Leutellier for having reviewed the English language.

## References

[1] J. Adamczyk, R. Dylewski, The impact of thermal insulation investments on sustainability  
500 in the construction sector, *Renewable and Sustainable Energy Reviews* 80 (2017) 421–429.  
doi:10.1016/j.rser.2017.05.173.

URL <http://www.sciencedirect.com/science/article/pii/S1364032117308031>

[2] L. Liu, H. Li, A. Lazzaretto, G. Manente, C. Tong, Q. Liu, N. Li, The development history and  
prospects of biomass-based insulation materials for buildings, *Renewable and Sustainable Energy  
505 Reviews* 69 (2017) 912–932. doi:10.1016/j.rser.2016.11.140.

URL <http://www.sciencedirect.com/science/article/pii/S1364032116308887>

[3] A. M. Papadopoulos, State of the art in thermal insulation materials and aims for future develop-

ments, *Energy and Buildings* 37 (1) (2005) 77–86. doi:10.1016/j.enbuild.2004.05.006.

URL <http://www.sciencedirect.com/science/article/pii/S0378778804001641>

- 510 [4] A. Torres-Rivas, M. Palumbo, A. Haddad, L. F. Cabeza, L. Jiménez, D. Boer, Multi-objective optimisation of bio-based thermal insulation materials in building envelopes considering condensation risk, *Applied Energy* 224 (2018) 602–614. doi:10.1016/j.apenergy.2018.04.079.

URL <http://www.sciencedirect.com/science/article/pii/S0306261918306378>

- 515 [5] M. Palumbo, A. M. Lacasta, M. P. Giraldo, L. Haurie, E. Correal, Bio-based insulation materials and their hygrothermal performance in a building envelope system (ETICS), *Energy and Buildings* 174 (2018) 147–155. doi:10.1016/j.enbuild.2018.06.042.

URL <http://www.sciencedirect.com/science/article/pii/S0378778817336654>

- [6] M. Zhang, M. Qin, C. Rode, Z. Chen, Moisture buffering phenomenon and its impact on building energy consumption, *Applied Thermal Engineering* 124 (2017) 337–345. doi:10.1016/j.applthermaleng.2017.05.173.

520 URL <http://www.sciencedirect.com/science/article/pii/S1359431117327989>

- [7] R. B. Glassco, R. L. Noble, Modular building construction and method of building assembly, international Classification E04B1/12, E04C2/16; Cooperative Classification E04C2/16; European Classification E04C2/16 (May 1987).

525 URL <http://www.google.fr/patents/W01987003031A1>

- [8] R.-C. Sun, J. Tomkinson, Appendix 1: Essential guides for isolation/purification of polysaccharides, in: *Encyclopedia of Separation Science*, Vol. 6, Academic Press, 2000, pp. 4568–4574. doi:10.1016/B0-12-226770-2/07271-9.

URL <https://www.sciencedirect.com/science/article/pii/B0122267702072719>

- 530 [9] F. Collet, S. Prétot, C. Lanos, Hemp-Straw Composites: Thermal And Hygric Performances, *Energy Procedia* 139 (2017) 294–300. doi:10.1016/j.egypro.2017.11.211.  
URL <http://www.sciencedirect.com/science/article/pii/S1876610217356229>
- [10] M. Viel, F. Collet, C. Lanos, Chemical and multi-physical characterization of agro-resources' by-product as a possible raw building material, *Industrial Crops and Products* 120 (2018) 214–237.  
535 doi:10.1016/j.indcrop.2018.04.025.  
URL <http://www.sciencedirect.com/science/article/pii/S0926669018303364>
- [11] M. Martelli-Tosi, O. B. G. Assis, N. C. Silva, B. S. Esposto, M. A. Martins, D. R. Tapia-Blácido, Chemical treatment and characterization of soybean straw and soybean protein isolate/straw composite films, *Carbohydrate Polymers* 157 (2017) 512–520. doi:10.1016/j.carbpol.2016.10.013.  
540 URL <http://www.sciencedirect.com/science/article/pii/S0144861716311729>
- [12] N. Mosier, C. Wyman, B. Dale, R. Elander, Y. Y. Lee, M. Holtzapple, M. Ladisch, Features of promising technologies for pretreatment of lignocellulosic biomass, *Bioresource Technology* 96 (6) (2005) 673–686. doi:10.1016/j.biortech.2004.06.025.  
URL <http://www.sciencedirect.com/science/article/pii/S0960852404002536>
- 545 [13] J. Song, C. Chen, S. Zhu, M. Zhu, J. Dai, U. Ray, Y. Li, Y. Kuang, Y. Li, N. Quispe, Y. Yao, A. Gong, U. H. Leiste, H. A. Bruck, J. Y. Zhu, A. Vellore, H. Li, M. L. Minus, Z. Jia, A. Martini, T. Li, L. Hu, Processing bulk natural wood into a high-performance structural material, *Nature* 554 (7691) (2018) 224–228. doi:10.1038/nature25476.  
URL <http://www.nature.com/doifinder/10.1038/nature25476>
- 550 [14] S.-Q. Tian, R.-Y. Zhao, Z.-C. Chen, Review of the pretreatment and bioconversion of lignocellulosic biomass from wheat straw materials, *Renewable and Sustainable Energy Reviews* 91 (2018) 483–

489. doi:10.1016/j.rser.2018.03.113.

URL <http://www.sciencedirect.com/science/article/pii/S136403211830203X>

[15] F. Rabier, Modélisation par la méthode des plans d'expériences du comportement dynamique d'un  
555 module IGBT utilisé en traction ferroviaire, PhD Thesis, Institut National Polytechnique, Toulouse  
(Sep. 2007).

URL <http://ethesis.inp-toulouse.fr/archive/00001595/>

[16] J. Goupy, L. Creighton, Introduction aux plans d'expériences, Dunod, Paris, 2006, oCLC:  
228784527.

560 [17] G. W. Oehlert, A first course in design and analysis of experiments, W.H. Freeman, New York,  
2000.

[18] AFNOR, NF EN ISO 12570 - Performance hygrothermique des matériaux et produits pour le  
bâtiment - Détermination du taux d'humidité par séchage à chaud (October 2000).

[19] ASTM, D854 - Standard test methods for specific gravity of soil solids by water pycnometer (May  
565 2014).

URL [www.astm.org](http://www.astm.org)

[20] BSI, BS EN 826:2013 Thermal insulating products for building applications - Determination of  
compression behaviour (May 2013).

[21] F. Collet, S. Pretot, Thermal conductivity of hemp concretes: Variation with formula-  
570 tion, density and water content, Construction and Building Materials 65 (2014) 612–619.  
doi:10.1016/j.conbuildmat.2014.05.039.

URL <http://linkinghub.elsevier.com/retrieve/pii/S0950061814005224>

- [22] C. Rode, R. H. Peuhkuri, L. H. Mortensen, K. K. Hansen, B. Time, A. Gustavsen, T. Ojanen, J. Ahonen, K. Svennberg, J. Arfvidsson, others, Moisture buffering of building materials, Tech. rep., Technical University of Denmark, Department of Civil Engineering (2005).
- 575
- [23] N. El Hajj, R. M. Dheilly, A. Goullieux, Z. Aboura, M. L. Benzeggagh, M. Quéneudec, Innovative agromaterials formulated with flax shaves and proteinic binder: Process and characterization, *Composites Part B: Engineering* 43 (2) (2012) 381–390. doi:10.1016/j.compositesb.2011.05.022.  
URL <http://www.sciencedirect.com/science/article/pii/S135983681100240X>
- [24] D. M. Nguyen, A.-C. Grillet, T. M. H. Diep, C. N. Ha Thuc, M. Woloszyn, Hygrothermal properties of bio-insulation building materials based on bamboo fibers and bio-glues, *Construction and Building Materials* 155 (2017) 852–866. doi:10.1016/j.conbuildmat.2017.08.075.  
580  
URL <http://www.sciencedirect.com/science/article/pii/S0950061817316665>
- [25] A. Bourdot, T. Moussa, A. Gacoin, C. Maalouf, P. Vazquez, C. Thomachot-Schneider, C. Bliard, A. Merabtine, M. Lachi, O. Douzane, H. Karaky, G. Polidori, Characterization of a hemp-based agro-material: Influence of starch ratio and hemp shive size on physical, mechanical, and hygrothermal properties, *Energy and Buildings* 153 (2017) 501–512. doi:10.1016/j.enbuild.2017.08.022.  
585  
URL <http://www.sciencedirect.com/science/article/pii/S0378778817312446>
- [26] R. V. Ratiarisoa, C. Magniont, S. Ginestet, C. Oms, G. Escadeillas, Assessment of distilled lavender stalks as bioaggregate for building materials: Hygrothermal properties, mechanical performance and chemical interactions with mineral pozzolanic binder, *Construction and Building Materials* 124 (2016) 801–815. doi:10.1016/j.conbuildmat.2016.08.011.  
590  
URL <http://linkinghub.elsevier.com/retrieve/pii/S0950061816312739>
- [27] E. Latif, S. Tucker, M. A. Ciupala, D. C. Wijeyesekera, D. Newport, Hygric properties of hemp

bio-insulations with differing compositions, *Construction and Building Materials* 66 (2014) 702–711.

doi:10.1016/j.conbuildmat.2014.06.021.

URL <http://www.sciencedirect.com/science/article/pii/S0950061814006369>

[28] C. Maalouf, B. S. Umurigirwa, N. Viens, M. Lachi, T. H. Mai, Study of the Hygric Behaviour and Moisture Buffering Performance of a Hemp–Starch Composite Panel for Buildings, *BioResources*

10 (1) (2014) 336–347. doi:10.15376/biores.10.1.336-347.